Combustion, Explosion, and Shock Waves, Vol. 45, No. 2, pp. 151–159, 2009

Ignition and Combustion of Magnesium Particles in a Nonuniform Thermal Field

A. V. Fedorov[1] **and A. V. Shul'gin**[1]

UDC 662.612:32

Translated from *Fizika Goreniya i Vzryva*, Vol. 45, No. 2, pp. 48–57, March–April, 2008.
Original article submitted March 20, 2008.

A distributed two-dimensional mathematical model of ignition and combustion of magnesium particles with allowance for the heterogeneous chemical reaction and for the region of the thermal influence of the particle on the gas is developed. Problems of particle ignition under the action of uniform and nonuniform thermal fields in a rectangular microchannel are solved.

Key words: ignition, combustion, heterogeneous chemical reaction, mathematical modeling.

INTRODUCTION

The problem of mathematical modeling of ignition and combustion of metal particles is of considerable interest for various branches of industry. Fedorov et al. [1] described mainly the pointwise and partly distributed models of ignition of small metal particles with low-temperature oxidation proceeding on the particle surface, the heat dissipated into the gas phase being ignored. This means that the thickness of the so-called "surrounding" film is negligibly small. A distributed mathematical model of magnesium-particle ignition with allowance for the heterogeneous chemical reaction and for the region of the thermal influence of the particle on the gas was developed in [2–4] in a one-dimensional formulation. In the present paper, the results obtained in [2–4] are generalized to the case of one-dimensional and two-dimensional mathematical models, which allows a realistic particle temperature after its ignition to be obtained. This is reached by using the concept about deceleration of some part of heterogeneous reactions proceeding on the particle surface when a certain limiting temperature T_m is reached [1]. It was necessary to develop a two-dimensional mathematical model because the subject under study was the influence of the shape of the gas region surrounding the particle on the processes of ignition and subsequent combustion. Note that the boundary of the gas layer in [2–4] was shaped as a circle.

[1]Khristianovich Institute of Theoretical and Applied Mechanics, Siberian Division, Russian Academy of Sciences, Novosibirsk 630090; fedorov@itam.nsc.ru; shulgin@itam.nsc.ru.

PHYSICOMATHEMATICAL FORMULATION OF THE PROBLEM

Let us consider a two-phase medium consisting of a magnesium particle of radius r_p ($R_p = \{-r_p \leqslant x, y \leqslant r_p\}$) located in a gas region $R_g = \{(x, y) \in (-L_x, L_x) \cup (-L_y, L_y) \backslash R_p\}$. The mathematical model that describes the temperature fields in the particle (T_2) and in the ambient gas (T_1) has the form

$$\rho_2 c_2 \frac{\partial T_2}{\partial t} = \lambda_2 \left(\frac{\partial^2 T_2}{\partial x^2} + \frac{\partial^2 T_2}{\partial y^2} \right), \ (x, y) \in R_p, \quad (1)$$

$$\rho_1 c_1 \frac{\partial T_1}{\partial t} = \lambda_1 \left(\frac{\partial^2 T_1}{\partial x^2} + \frac{\partial^2 T_1}{\partial y^2} \right), \ (x, y) \in R_g, \quad (2)$$

where ρ_i, λ_i, and c_i are the densities, thermal conductivities, and specific heats of the gas ($i = 1$) and the particle ($i = 2$). Equations (1) and (2) have to satisfy the initial condition

$$T_1(x, y, 0) = T_{01}(x, y), \quad T_2(x, y, 0) = T_{02}(x, y), \quad (3)$$

the condition of heat transfer on the boundary of the gas region

$$\lambda_1 \boldsymbol{n} \cdot \nabla T_1(x, y, t) = -\alpha (T_1(x, y, t) - T_c(x, y)), \quad (x, y) \in \partial R_g, \quad (4)$$

and the boundary conditions on the interface

$$T_2(x,y,t) = T_1(x,y,t), \quad (x,y) \in \partial R_p, \tag{5}$$

$$\lambda_2 \boldsymbol{n} \cdot \nabla T_2(x,y,t) = \lambda_1 \boldsymbol{n} \cdot \nabla T_1(x,y,t) + q_0 \rho_3 f(T_m, T_2) K \exp\left[-\frac{E}{RT_2(x,y,t)}\right], \quad (x,y) \in \partial R_p, \tag{6}$$

where q_0 is the specific heat release per oxide mass, ρ_3 is the oxide density, K is the preexponent in the oxidation law, E is the activation energy of low-temperature oxidation, R is the universal gas constant, $\alpha = \mathrm{Nu}/2$ is the coefficient of heat transfer between the particle and the gas, Nu is the Nusselt number, T_c is the temperature on the boundary of the gas region, and $f(T_m, T_2) = 1$ (model 1) or $f(T_m, T_2) = T_m - T_2$ (model 2) (T_m is a certain limiting temperature).

Let us introduce the following dimensionless variables and parameters:

$$\bar{x} = \frac{x}{r_p}, \ \bar{y} = \frac{y}{r_p}, \ \bar{T}_i = \frac{T_i}{T_0}, \ \bar{T}_c = \frac{T_c}{T_0}, \quad \bar{L}_x = \frac{L_x}{r_p}, \ \bar{L}_y = \frac{L_y}{r_p}, \ \bar{\alpha} = \alpha \frac{r_p}{\lambda_1}; \tag{7}$$

$$\bar{t} = t \frac{\lambda_2}{\rho_2 c_2 r_p^2} = \frac{t}{t_0}, \ t_0 = \frac{\rho_2 c_2 r_p^2}{\lambda_2}, \quad \bar{C}_1 = \frac{\lambda_1}{\lambda_2} \frac{\rho_2}{\rho_1} \frac{c_2}{c_1}, \ \bar{\lambda} = \frac{\lambda_2}{\lambda_1}, \ \bar{E} = \frac{E}{RT_0}; \tag{8}$$

$$\bar{q}_0 = \frac{q_0 \rho_3 K r_p}{\lambda_1 T_0} \quad \text{(model 1)}, \qquad \bar{q}_0 = \frac{q_0 \rho_3 K r_p}{\lambda_1} \quad \text{(model 2)}. \tag{9}$$

Omitting the bar over the dimensionless variables, we write the final formulation of the problem:

$$\frac{\partial T}{\partial t} + \mathrm{div}(-k \nabla T) = 0, \tag{10}$$

$$T(x,y,0) = T_0(x,y,0), \tag{11}$$

$$\boldsymbol{n} \cdot \nabla T(x,y,t) = -\alpha (T(x,y,t) - T_c(x,y)), \quad (x,y) \in \partial R_g, \tag{12}$$

$$\lambda \boldsymbol{n} \cdot \nabla T_+(x,y,t) = \boldsymbol{n} \cdot \nabla T_-(x,y,t) + q_0 f(T_m, T_2) \exp\left[-\frac{E}{T(x,y,t)}\right], \quad (x,y) \in \partial R_p. \tag{13}$$

Here $k = 1$ in the particle region and $k = C_1$ in the gas region; the plus and minus subscripts in Eq. (13) indicate the interface values on the side of the particle and the gas, respectively. The values of the physicomechanical parameters were given in [2]. Problem (10)–(13) was solved numerically by the FlexPDE software package [5].

DISCUSSION OF NUMERICAL RESULTS

Testing

To estimate results computed by the FlexPDE software package, we performed test computations and compared the results with the data [2, 3] obtained by the finite-difference method in a one-dimensional formulation. For this purpose, we assumed that the gas region R_g is a ring with an outer radius L, with a condition of uniform heat transfer of the type (12) being imposed on the boundary: $\boldsymbol{n} \cdot \nabla T = -\alpha(T - T_c)$.

In accordance with the theory developed in [1, 3], the catastrophe manifold in the problem considered is determined by the relations

$$\beta = \frac{\alpha L^\nu / q_0}{1 + \dfrac{\alpha L}{\nu - 1} - \dfrac{\alpha L^\nu}{\nu - 1}} = \frac{f(T_m, T_2)}{T_2 - T_c} \exp\left(-\frac{E}{T_2}\right) \tag{14}$$

($\nu = 0$ and 2 for the Cartesian and spherical coordinates, respectively), and the turning points of the catastrophe manifold are determined by the expression

$$T_2^{\pm} = \frac{E}{2}\left(1 \pm \sqrt{1 - \frac{4T_c}{E}}\right) \tag{15}$$

for model 1 and by the expression

$$T_2^{\pm} = \frac{E(T_m + T_c)}{2(E + T_m - T_c)} \times \left[1 \pm \sqrt{1 - \frac{4T_m T_c (E + T_m - T_c)}{E(T_m + T_c)^2}}\right] \tag{16}$$

for model 2. It follows from Eqs. (15), (16) that the condition $E \geqslant E_{\min}$ should be satisfied, where $E_{\min} = 4T_c$ for Eq. (15) and $E_{\min} = 4T_m T_c/(T_m - T_c)$ for Eq. (16). As was shown in [1, 2], for $\beta \geqslant \beta_-$, there exists a solution $T_2 \in [T_-, T_c]$, which describes the regime of regular heating. For $\beta_- \leqslant \beta \leqslant \beta_+$, the existing solution $T_2 \in [T_-, T_+]$ corresponds to the unstable heating regime. Finally, for $0 \leqslant \beta \leqslant \beta_-$, the solution $T_2 \geqslant T_-$ is on the ignition manifold branch corresponding to the phenomenological criterion of ignition. Here, $\beta_\pm$ indicates the values of this quantity calculated at the turning points, i.e., for $T_2 = T_2^\pm$.

Regular Heating Regime. Let us choose $\beta \geqslant \beta_-$ and $T_c = 1122$ K. We solve the problem of reaching a steady (without ignition) regime of heating of a magnesium particle of radius $r_p = 17$ μm for a gas region whose length equals two particle radii. The problem is solved in a one-dimensional formulation by virtue of the formulation symmetry by the method developed in [2] and in a two-dimensional formulation by the FlexPDE software package. The maximum difference between the computed results is less than 1%; in particular, the value

TABLE 1

Ignition Delay for $\beta < \beta_-$

$\beta \cdot 10^5$	t_{ign}, msec
3.95029	110.9
3.64849	78.0
3.34182	65.2
3.03025	48.2
2.71374	41.4
2.39227	36.2
2.06579	31.9
1.73427	28
1.39769	24.8
1.05600	21.6
0.70918	18.4
0.35719	14.8

of temperature at the point $L = 2$ is 3.80 (FlexPDE) and 3.79 (one-dimensional problem).

Ignition Regime. Let us choose $\beta < \beta_-$. The parameter q_0 is calculated in accordance with Eq. (14):

$$q_0 = \frac{1}{\beta} \frac{\alpha L^\nu}{1 - \dfrac{\alpha L}{\nu - 1} + \dfrac{\alpha L^\nu}{\nu - 1}}. \qquad (17)$$

Let $L = 2$, $r_p = 17$ μm, $T_c = 1122$ K, and $T_m = 2T_c$. The ignition delays t_{ign} calculated by model 2 in a one-dimensional formulation for $\beta < \beta_- = 4.23083 \cdot 10^{-5}$ are listed in Table 1. In calculations by model 1 with $\beta = \beta_2 = 8.2035 \cdot 10^{-6}$ ($\beta_1 = 7.09181 \cdot 10^{-6} < \beta_2 < \beta_3 = 1.05600 \cdot 10^{-5}$; see Table 1), we obtain $t_{\text{ign}} = 20.9$ msec. The difference between the values of t_{ign} calculated by models 1 and 2 is approximately 3%.

Table 2 gives the ignition delays t_{ign} as functions of the gas-region size L, which were obtained by the method developed in [2] (columns 2–4) and by the finite-element method (FEM) (column 5; FlexPDE software). The data calculated by model 1 with $\beta = \beta_2$ (data [2]) are given in column 2, and the data calculated by model 2 with $\beta = \beta_3$, $\beta = \beta_1$, and $\beta = \beta_2$ are listed in columns 3–5, respectively. A comparison of these data shows that the ignition delays calculated by different methods coincide within ≈0.6%. Moreover, these times calculated by different models are also close to each other. Model 2 offers an advantage of determining a physically realistic value of the particle temperature after its ignition. Note also that the values of t_{ign} in columns 2–4 of Table 2 were obtained under the condition $\beta_1 < \beta_2 < \beta_3$, i.e., an estimate of the ignition delay

TABLE 2

Ignition Delay versus the Gas-Region Size

L	t_{ign}, msec			
	Model 1 $\beta = \beta_2$	Model 2		
		$\beta = \beta_3$	$\beta = \beta_1$	$\beta = \beta_2$ (FEM)
2	20.9	21.6	18.4	21
4	23.2	23.4	19.8	23.2
6	24.6	24.8	21.2	24.55
8	25.2	25.8	22	25.6
10	25.6	26.5	22.7	26.4

Note. The data for model 1 marked by an asterisk were obtained in [2].

TABLE 3

Ignition Delay versus the Particle Radius

r_p, μm	t_{ign}, msec			
	Method of [2]		FEM	
	$T_c =$ 1122 K	$T_c =$ 1538 K	$T_c =$ 1122 K	$T_c =$ 1538 K
17	21.6	8.5	21	7.9
20	29.9	11.78	29.2	11.2
30	67.35	26.5	66.8	26
40	119.7	47.1	119.1	46.6
50	187.1	73.6	186.7	73.2
60	269.4	106	268.6	105.4

for model 1 is really obtained. For instance, for $L = 2$, we have $18.4 < 20.9 < 21.6$ msec.

The ignition delays versus the particle radius, calculated by model 2 with $\beta = \beta_3$, $L = 2$, $T_c = 1122$ K, and $T_c = 1538$ K, are listed in Table 3 and plotted in Fig. 1. The calculations were performed by the method developed in [2] and by the FEM. It is seen that the ignition delay increases with increasing particle radius and decreases with a fixed particle radius and increasing ambient temperature, as it could be expected.

Thus, the results calculated by models 1 and 2 as functions of the parameters L, r_p, and β are in reasonable agreement with each other. Moreover, as was indicated earlier in [2–4], the computed ignition delays agree with experimental data. After testing of the computational method, let us discuss the results obtained further by model 2.

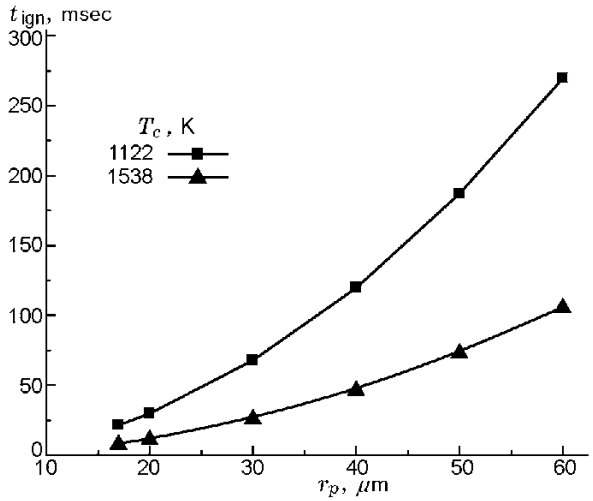

Fig. 1. Ignition delay versus the particle radius.

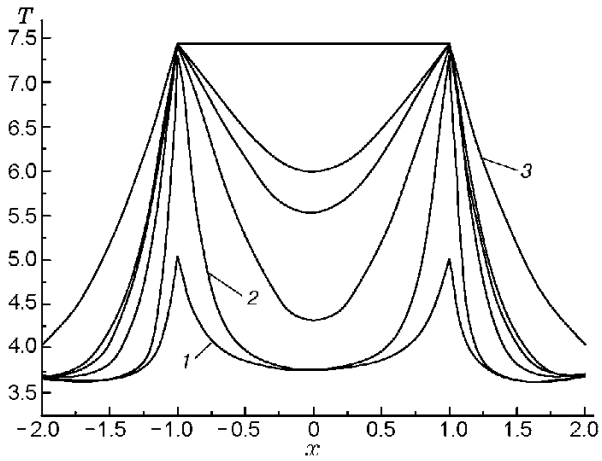

Fig. 2. Dynamics of the temperature field in the particle–gas system.

Uniform and Nonuniform Heating in a Rectangular Microregion

Single Particle. Let the gas region R_g be a square with sides $L_x = L_y = 2$, and let the particle be located at the center of the region considered. For $r_p = 17$ μm and $T_c = 1122$ K, the one-dimensional model predicts the ignition delay to be 21 msec , while the two-dimensional model predicts the ignition delay to be 21.5 msec (for the circular region of the gas surrounding the particle; the difference in ignition delays is ≈2%) and 23.5 msec (for the square region of the gas surrounding the particle; the difference in ignition delays is about 11%). The area of the gas layer increased by 25% thereby. The increase in the ignition delay caused by the transition from the circular to the square region can be physically explained by the increase in the ambient gas volume, which necessitates longer heating.

Let us now consider nonuniform heating. Let the boundary conditions on the gas-region boundary have the form

$$\begin{gathered} \boldsymbol{n}\cdot\nabla T(\pm L_x, y, t) = -\alpha(T(\pm L_x, y, t) - T_c), \\ -L_y \leqslant y \leqslant L_y, \\ \boldsymbol{n}\cdot\nabla T(x, \pm L_y, t) = -\alpha(T(x, \pm L_y, t) - T_{c1}), \\ -L_x \leqslant x \leqslant L_x, \end{gathered} \tag{18}$$

where $T_c = 1122$, 1300, and 1500 K on the vertical boundaries of the gas region, and the temperature T_{c1} on the horizontal boundaries was chosen to be lower than the critical temperature of ignition equal to ≈950 K in the case considered [4].

Figure 2 illustrates the dynamics of the temperature field in the particle–gas system over the cross section $-L_x \leqslant x \leqslant L_x$, $y = 0$ for the case with $T_c = 1122$ K and $T_{c1} = 900$ K. Curve 1 corresponds to the beginning of the drastic increase in temperature on the particle boundary. Curve 2 shows the instant of ignition, which was determined by the criterion $|T - T_m| \leqslant \varepsilon$ ($t = 32.6$ msec), and curve 3 shows the instant when the temperature in the entire particle region reaches the limiting value ($t = 35.16$ msec). The curves located between curves 2 and 3 illustrate the dynamics of heating. As it follows from the data in Fig. 2, particle ignition begins when the gas temperature in the vicinity of the particle boundary reaches and slightly exceeds the limiting ignition temperature, which is ≈950 K in the case considered. The level lines of the temperature field of the system corresponding to curves 2 and 3 are shown in Fig. 3. Note that the ignition occurs simultaneously on the entire particle surface in the case of uniform heating; in the case of nonuniform heating, however, the ignition begins on those parts of the particle surface that are located closer to the hotter boundaries of the gas region. After the particle temperature reaches the limiting value, the temperature distribution in the system becomes close to uniform within a distance approximately equal to one half of the particle radius; the temperature distribution in the remaining region is substantially nonuniform (Fig. 3b).

Figure 4 shows the behavior of the ignition delay as a function of the temperature T_{c1} on the horizontal boundaries of the square gas region $L_x = L_y = 2$. It is seen that the ignition delay increases with decreasing T_{c1}; as the temperature T_{c1} reaches a certain minimum value (600, 400, and 200 K in the variants considered), no ignition occurs, and the regular heating regime is achieved. As T_{c1} increases, the curves come closer to each other, and the limiting ignition delay for each curve corresponds to its value at $T_{c1} = T_c$ (at

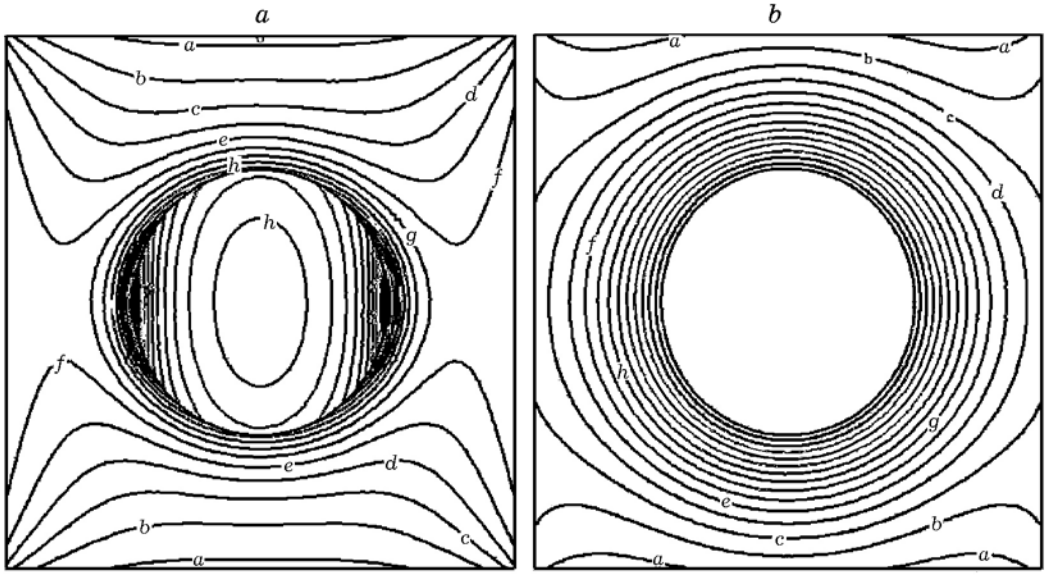

Fig. 3. Level lines of the temperature field of the particle–gas system: $t = 32.6$ (a) and 35.16 msec (b).

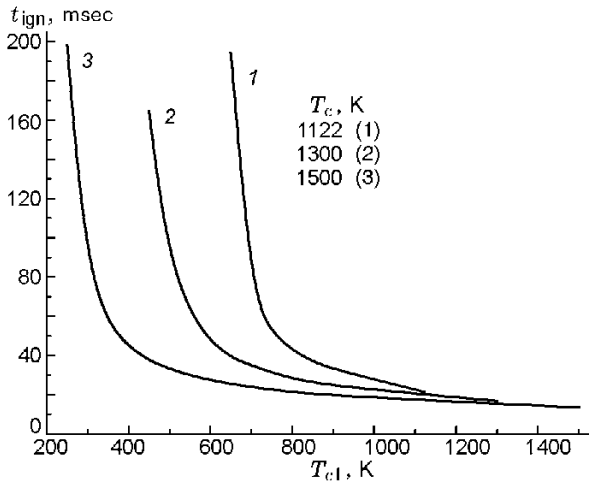

Fig. 4. Behavior of the ignition delay versus the temperature T_{c1}.

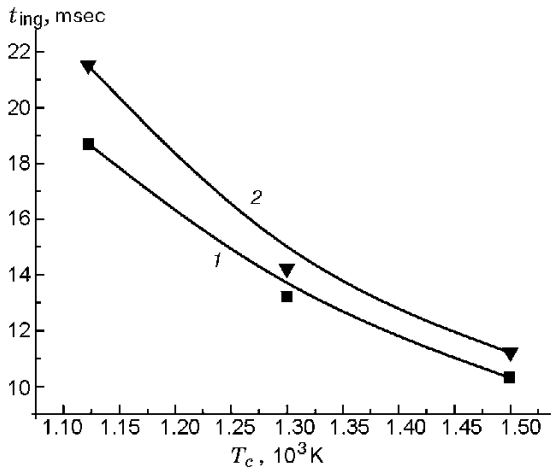

Fig. 5. Ignition delay versus the temperature on the gas-region boundary for a square region (1) and for a circular region (2).

$T_{c1} = 1122$, 1300, and 1500 K, we have $T_{\rm ign} = 23.5$, 16.9, and 13.4 msec, respectively).

Let us introduce the notion of the averaged temperature of the gas-region boundary $\langle T\rangle = \sum\limits_i S_i T_{ci} / \sum\limits_i S_i$, where T_{ci} is the temperature on the ith boundary and S_i is the area of the ith boundary. As it follows from the calculations performed, the condition of ignition in all three variants is $\langle T\rangle > 875$ K. This value agrees with the critical ignition temperature $T_{\rm cr}$ within ≈8%. Thus, the averaged temperature $\langle T\rangle$ can serve as the ignition criterion under the conditions of nonuniform heating as well, namely, the particle ignition occurs if $\langle T\rangle > T_{\rm cr}$.

It seems of interest to continue studying the effect of the size of the gas region surrounding the particle on the ignition delay. Let $S_{\rm sq}$ and $S_{\rm circ}$ be the areas of the square and circular gas regions. For the condition of identical areas $S_{\rm sq} = S_{\rm circ}$ (volumes) to be satisfied, it is necessary to impose the condition $L_x = L_y = \sqrt{\pi}$. In this case, for $T = 1122$, 1300, and 1500 K, we have $t_{\rm ign} = 18.7$, 13.2, and 10.3 msec for the square gas region (curve 1 in Fig. 5) and $t_{\rm ign} = 21.5$, 14.2, and 11.2 msec for the circular gas region (curve 2 in Fig. 5). It can be noted that the ignition delays become closer to each other as the initiating temperature increases. This is consistent with the physical fact that the increase in

the gas-region size becomes insignificant at high temperatures.

In the problem of ignition with cylindrical symmetry, we managed to find the coefficient of the transition to the ignition problem in the planar formulation in terms of the parameter t_{ign}. If the rectangle sizes are taken as $L_x = L_y \approx 1.85$, it is possible to obtain identical values of t_{ign}. This means that the values of t_{ign} in calculations of particle heating in the cylindrical and planar approximations are identical. The area of the equivalent square [cross section of the channel where the particle (filament) is located] can be recalculated with respect to the area of the cylindrical channel in the form $S_{\text{sq}}/S_{\text{circ}} = 1.85\sqrt{\pi}$. This relation remains valid for different sizes of the gas region and temperatures on the boundaries of this region. In particular, retaining this relation and changing the initiating temperature at $T_c = 1300$ K, we obtain $t_{\text{ign}} = 6.59$ msec for the square gas region and $t_{\text{ign}} = 6.46$ msec for the cylindrical gas region; at $T_c = 1500$ K, we have $t_{\text{ign}} = 5.05$ msec for the square gas region and $t_{\text{ign}} = 4.94$ msec for the cylindrical gas region. In addition, a calculation was performed with doubled sizes of the corresponding regions. In this case, the ignition delay is 20.16 msec in the square gas region and 19.8 msec in the cylindrical gas region at a fixed temperature $T_c = 1500$ K. It is seen that the difference is insignificant. Thus, the notion of the equivalent cylindrical layer in this range of ambient temperatures and gas-region sizes is introduced and verified by calculations.

Two Particles. Let us consider a square gas region of size $L_x = L_y = 4$ containing two particles of an identical size; the coordinates of the particle centers are $(\pm L_x/2, 0)$. The condition of uniform heat transfer with a temperature $T_c = 1122$ K is imposed on the entire boundary of the gas region. In this case, the ignition delay is 21.55 msec instead of 26.5 msec in the same gas region with one particle at the center. The shorter ignition delay here is caused by the fact that the particles are located closer to the side boundaries of the gas region and by their thermal interaction. Figure 6 shows the temperature distribution in the system over the cross section $-L_x \leqslant x \leqslant L_x$, $y = 0$ at the instant of ignition. The temperature distribution at the instant of ignition is seen to be rather nonuniform. The temperature on the back sides of both particles is much lower than the temperature on the frontal sides of the particles. Thus, there is a temperature gradient in the temperature field.

Let us now consider nonuniform heating of a system containing two particles and the gas by imposing the heat-transfer condition $\boldsymbol{n} \cdot \nabla T = -\alpha(T - T_c)$ on the right vertical boundary of the gas region $x = L_x$, $-L_y \leqslant y \leqslant L_y$ and the condition $\boldsymbol{n} \cdot \nabla T = 0$ on the remaining boundaries. In this case, the right particle is ignited earlier [this particle is closer to the right boundary; see Fig. 7 (temperature distribution in the cross section $-L_x \leqslant x \leqslant L_x$, $y = 0$; curve 1)]; its ignition delay is 68.24 msec. After a certain time, the second particle is ignited; its ignition delay is 79.12 msec (curve 2 in Fig. 7); during this time, the first particle reaches the steady value of temperature $T \approx T_m$. Thus, the relay mechanism of ignition, which was previously observed within the framework of the pointwise approach [6, 7], is also realized here.

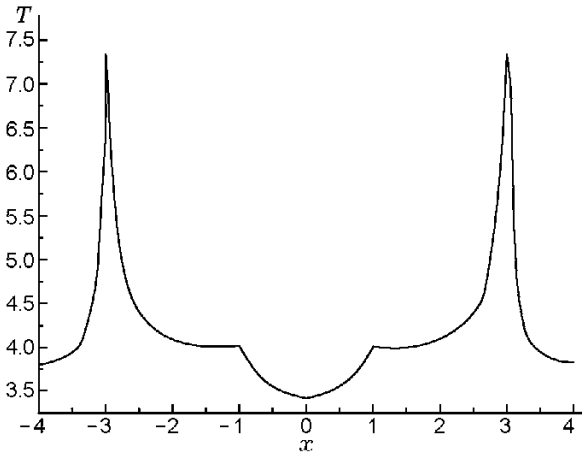

Fig. 6. Temperature distribution in the system containing two particles and the gas at the instant of ignition in the case of uniform heating.

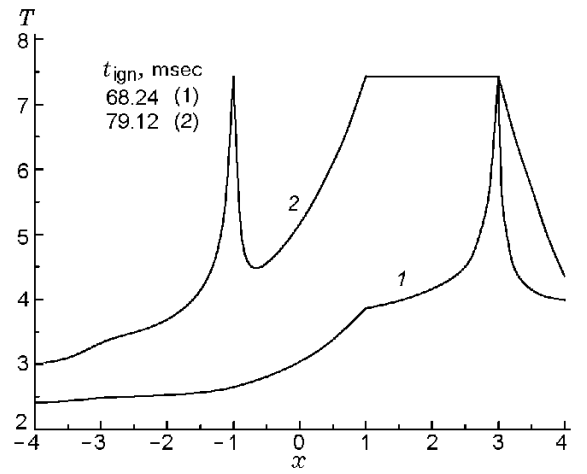

Fig. 7. Temperature distribution in the system containing two particles and the gas at the instant of ignition in the case of nonuniform heating.

Let us now study the influence of the relative positions of two particles on the ignition delay. For this purpose, we consider the previous problem of nonuniform

TABLE 4

Ignition Delay of Two Particles versus the Distance between Them

Δx	t_{ign1}, msec	t_{ign2}, msec	
		with no allowance for combustion	with allowance for combustion
1	91.4	95.5	92.82
2	88.4	104.2	97.25
3	86.2	119.7	298
4	85.1	139.7	429
5	84	163.8	558
6	83.5	191.8	—
7	83.3	223.5	—
8	83.2	258.8	—
9	83.1	297.4	—

heating in a rectangular region with the sizes $L_x = 20$ and $L_y = 4$. The first particle is located at a distance of one radius from the right boundary of the gas region, where the heating is provided, and the second particle is located at a distance Δx from the left boundary of the first particle. The ignition delays for the first (t_{ign1}) and second (t_{ign2}) particles calculated for different values of Δx are plotted in Fig. 8 and summarized in Table 4. The ignition delay of the first particle decreases from 91.4 msec at $\Delta x = 1$ to 83.1 msec at $\Delta x = 9$ and remains unchanged with a further increase in Δx. Vice versa, the ignition delay of the second particle continuously increases with increasing Δx. The value of the ignition delay of the first particle here is greater than that in the previous problem of heating with the square gas region, which is attributed to the increase in the total gas volume.

The increase in the ignition delay of the first particle for moderate values of Δx is caused by the fact that some part of the incoming heat is spent on heating the second particle (the specific heat of the particle material is substantially higher than the specific heat of the gas); the greatest effect on the ignition delay of the first particle is observed at $\Delta x \leqslant 4$–5. Thus, our conclusion [2] that the characteristic size of the region of particle influence on the ignition delay can be assumed to be equal to 4 to 5 particle radii is validated for the first particle. Curves 1 and 2 in Fig. 8 can be approximately described by the dependences $t_{\text{ign1}} = 94.38 - 3.44\Delta x + 0.27\Delta x^2$ and $t_{\text{ign2}} = 88.65 + 3.86\Delta x + 2.21\Delta x^2$.

It should be noted, however, that the data on the ignition delay for the second particle are obtained under the condition that the heat is generated by the ignition process only.

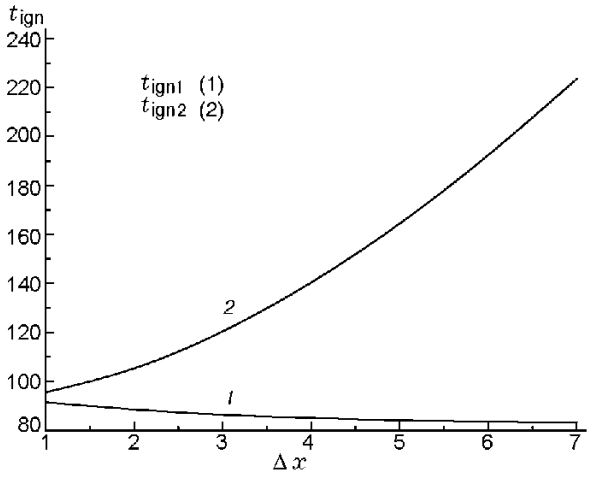

Fig. 8. Ignition delay of two particles versus the distance between them.

Let us now study the ignition with allowance for the combustion process. Assuming that the particle retains its spherical shape during combustion and decreases in size, we write the law for the decrease in the particle radius with time in dimensionless variables as

$$r = \sqrt{1 - \gamma t}, \tag{19}$$

where γ is a certain constant. Relation (19) follows from the so-called law of d^2. The boundary condition on the interface (13) acquires the form

$$\lambda \boldsymbol{n} \cdot \nabla T_2(x, y, t) = \boldsymbol{n} \cdot \nabla T_1(x, y, t)$$

$$- q_b(T_b - T_2)\frac{dr}{dt}, \ (x, y) \in \partial R_p, \tag{20}$$

or, with allowance for Eq. (19),

$$\lambda \boldsymbol{n} \cdot \nabla T_2(x,y,t) = \boldsymbol{n} \cdot \nabla T_1(x,y,t) + q_b(T_b - T_2)\frac{\gamma}{2r}, (x,y) \in \partial R_p, \qquad (21)$$

where $q_b > q_0$ and $T_b > T_m$. Here T_b has the meaning of the burning temperature. The second term in the right side of equality (20) corresponds to heat supply due to the combustion reaction. The function $r(x(t), y(t))$ decreasing with time is a function that describes the empirical law of combustion, as was mentioned above.

We can obtain an analog of the catastrophe manifold under condition (21) for a one-dimensional problem in a steady case by using the procedure described in [2]. It has the following form:

$$\beta = \frac{\alpha L^\nu / q_0}{1 - \dfrac{\alpha L}{\nu - 1} + \dfrac{\alpha L^\nu}{\nu - 1}} = \frac{T_b - T_2}{T_2 - T_c}\frac{\gamma}{2r}, \qquad (22)$$

$$T_2 = \frac{q_0 T_b \gamma / 2r + A T_c}{q_0 \dfrac{\gamma}{2r} + A}, \; A = \frac{\alpha L^\nu}{1 - \dfrac{\alpha L}{\nu - 1} + \dfrac{\alpha L^\nu}{\nu - 1}}. \qquad (23)$$

It follows from Eq. (23) that $\lim\limits_{r \to 0} T_2 = T_b$, i.e., the particle temperature tends to T_b as the particle burns out.

Let us illustrate the solution of the problem of ignition and combustion of a single particle with the parameters $q_b = 1.5 q_0$ and $T_b = 1.5 T_m$. The mathematical model can be formulated as follows. At the first stage, we solve problem (10)–(13), which describes particle ignition with the heat-transfer condition $\boldsymbol{n} \cdot \nabla T = -\alpha(T - T_c)$ on the right vertical boundary of the gas region $x = L_x$, $-L_y \leqslant y \leqslant L_y$ and with the condition $\boldsymbol{n} \cdot \nabla T = 0$ on the other boundaries. After the system is ignited, we solve the boundary-value problem with condition (21) on the contact, i.e., the temperature distribution in the system is fixed at the instant of ignition. The instant of ignition is determined by the criterion $T(0,0) \geqslant 0.9 T_m$ in solving the ignition problem. This distribution is shown in the cross section $-L_x \leqslant x \leqslant L_x$, $y = 0$ in Fig. 9 (curve 1). Then, a new calculation with new parameters of the model corresponding to combustion is performed. Curve 2 in Fig. 9 shows the temperature distribution in the system at the time when the particle surface reaches a temperature close to the burning temperature T_b, which is further denoted by T_b'. Then, the particle radius decreases (the particle burns out), and simultaneously the temperature in the region occupied by the particle increases to the limiting value T_b' (curve 3 in Fig. 9). During this time interval, particle burnout at this temperature occurs until the calculation is terminated in accordance with the criterion $r \leqslant 0.1 r_0$ (curve 4 in Fig. 9). The

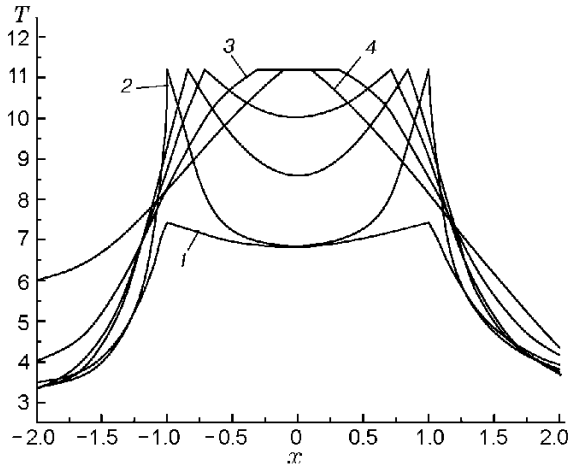

Fig. 9. Dynamics of the temperature field in the particle–gas system with allowance for combustion.

burning time for $\gamma = 0.5$ is $t_b = 1.47$ msec, which agrees with experimental data [8]. Note that the adiabatic wall condition is imposed on all boundaries, except for the right boundary, which results in an asymmetric increase in temperature on these walls.

Let us now consider the case with two particles located in the region $L_x = 20$, $L_y = 4$ at a distance Δx from each other. We assume that particle burning leaves a coke remainder in the form of a small-size particle with 10% of the initial particle size. For simplicity, the thermophysical variables of the coke remainder are assumed to be identical to those of the unburned particle. As no heat is further produced owing to combustion, then the boundary condition (21) is replaced by the condition of identical heat fluxes $\boldsymbol{n} \cdot \nabla T_2 = \boldsymbol{n} \cdot \nabla T_1$ (the particle passes to the inert regime). The ignition delays of the first and second particles calculated by the model that ignores the combustion of the first particle are given in Table 4 (second and third columns), and the ignition delays of the second particle with allowance for the combustion of the first particle are listed in the last column.

We should note that the first model of ignition, which ignores coke cooling, predicts a substantially shorter ignition delay than the second model, which takes coke cooling into account. Nevertheless, the dependences $t_{\text{ign}}(\Delta x)$ are qualitatively similar; they both increase with increasing distance between the particles. In the interval of distances $\Delta x \in (2, 3)$, there is a critical value Δx_* after which the time t_{ign} changes catastrophically, i.e., the capability of the second particle to ignition is violated.

This phenomenon is caused by the concentration limit of ignition with the following mechanism. As the distance between the particle increases, the amount of

TABLE 5

Ignition Delays of Two Particles of Different Sizes versus the Distance between Them

Δx	t_{ign1}, msec	t_{ign2}, msec	$t_{\text{ign2}}^{\text{eq}}$, msec	$\frac{\Delta t_{\text{ign2}}}{t_{\text{ign2}}^{\text{eq}}} \cdot 100$ %
1	85.9	87.31	92.82	5.91
2	84.9	95.06	97.25	2.25
3	84.3	292.77	298	1.75

released heat becomes insufficient for the gas phase of the mixture to be heated; hence, the second particle occurs in a medium with an insufficient temperature for ignition. As a result, its ignition delay increases catastrophically.

Let us consider the effect of the particle size on the ignition and combustion processes. Let the radius of the first particle (which is closer to the right heated boundary of the microchannel $L_x = 20$, $L_y = 4$) be equal to unity, and let the radius of the second particle be 0.5. The calculated ignition delays for the first (t_{ign1}) and second (t_{ign2}) particles are listed in Table 5. If we compare these ignition delays with the ignition delays of the particles of an identical radius (see $t_{\text{ign2}}^{\text{eq}}$ in Table 5), we can see that the ignition delay of the second particle is not much shorter. The difference decreases with increasing distance between the particles. This may mean that the role of the particle size becomes less important with increasing distance between the particles; probably, the process of ignition of gas suspensions is controlled by the distance between the particles or by the concentration of particles in a cloud of particles.

Let now the radii of the first and second particles be equal to 1 and 2, respectively. Let us determine the mass concentration of particles by the formula $m_2 = \pi(r_1^2 + r_2^2)/(4L_xL_y)$. The calculations show that we have $t_{\text{ign1}} = 97.7$ msec, $t_{\text{ign2}} = 97.7 + 1.47 + 158 = 257.17$ msec, and $m_2 = 0.049$ for the region with $L_x = 20$, $L_y = 4$ and $t_{\text{ign1}} = 100.6$ msec, $t_{\text{ign2}} = 100.6 + 1.47 + 279 = 381.07$ msec, and $m_2 = 0.0245$ for the region with $L_x = 20$, $L_y = 8$. These results are consistent with the previously obtained data [9], which imply that the ignition delay increases with decreasing mass concentration of particles.

CONCLUSIONS

The following results were obtained by means of numerical implementation of a new two-dimensional mathematical model of ignition and combustion of small metal particles in microregions:

- The notion of the critical temperature of ignition is justified for a particle under conditions of nonuniform heating;
- In sufficiently long microchannels, the region of the united thermal influence of two identical particles is estimated as 4 to 5 particle radii;
- The law of similarity is valid for the thermal histories of particles located in a cylindrical channel and in a rectangular channel, with a certain coefficient of similarity of the domains for different physicochemical parameters;
- The mathematical model developed offers a qualitative description of the concentration limit of ignition and makes it possible to put forward an idea about its mechanism.

This work was supported by the Russian Foundation for Basic Research (Grant No. 06-01-00299).

REFERENCES

1. A. V. Fedorov, V. M. Fomin, and Yu. A. Gosteev, *Dynamics and Ignition of Gas Suspensions* [in Russian], Novosibirsk State Technical University, Novosibirsk (2006).
2. A. V. Fedorov and A. V. Shul'gin, "Conjugate mathematical model of ignition of magnesium samples," *Combust., Expl., Shock Waves*, **42**, No. 3, 295–301 (2006).
3. A. V. Fedorov and A. V. Shulgin, "About stability of the ignition process of small solid particle," *J. Loss Prevention in the Process Industries*, **20**, Nos. 4–6, 317–321 (2007).
4. V. N. Popov, A. V. Fedorov, and A. V. Shul'gin, "Numerical simulation of magnesium particle ignition in a nonuniform heat field," *Mat. Model.*, **19**, No. 6, 109–117 (2007).
5. http://www.pdesolutions.com.
6. Yu. A. Gosteev and A. V. Fedorov, "Discrete-continual model of flame propagation in a gas suspension of metal particles. I. One-dimensional approximation," *Combust., Expl., Shock Waves*, **41**, No. 2, 190–201 (2005).
7. Yu. A. Gosteev, A. V. Fedorov, and A. V. Shul'gin, "Discrete-continual model of flame propagation in a gas suspension of metal particles. II. Allowance for the pre-flame oxidation reaction," *Combust., Expl., Shock Waves*, *ibid.*, pp. 202–205.
8. V. P. Grachukho, E. S. Ozerov, and A. A. Yurinov, "Burning of magnesium particles in water vapor," *Combust., Expl., Shock Waves*, **7**, No. 2, 195–198 (1971).
9. A. V. Fedorov, "Ignition of gaseous suspensions in an interacting continuum regime," *Combust., Expl., Shock Waves*, **34**, No. 4, 418–425 (1998).